Rational Design of Effective Mg Degradation Modulators

C. Feiler,[‡,*] D. Mei,[*] B.J.C. Luthringer-Feyerabend,[**,*] S.V. Lamaka,[*] and M.L. Zheludkevich[**,*]

Prerequisite to unlock the full potential of Mg-based materials is to gain control of their degradation properties. Here a proof of concept is presented for an efficient and robust alternative to the data-driven machine learning approaches that are currently on the rise to facilitate the discovery of corrosion modulating agents. The electronic properties of bipyridine were tuned by its substitution with electron donating and electron withdrawing functional groups to regulate the degradation modulators interaction with different ions and the effect on the corrosion inhibition of pure Mg was predicted based on density functional theory calculations. Bipyridine and two of its derivatives were subsequently investigated experimentally to validate the trend predicted by the quantum chemical calculations.

KEY WORDS: degradation, density functional theory, magnesium, tailored inhibition

INTRODUCTION

The degradation behavior of magnesium (Mg) renders it one of the most versatile engineering materials available today as it can be used in a large variety of applications ranging from automotive[1-4] and aerospace components[5-7] as well as medical implants[8-11] to clean energy storage systems,[12-14] where Mg can be utilized as anode material. A prerequisite to unlock the full potential of Mg-based materials is gaining control over the corrosion rate, as each target implementation demands degradation properties specific to the field of application.[15-17] For transport applications, corrosion needs to be prevented to avoid material failure, while a constant degradation of the anode material in Mg-air primary batteries is required for battery application. A major advantage of Mg-based implants is that they will dissolve over time, rendering additional surgeries to remove implants from the patient obsolete. However, different injuries impose different healing times and the degradation rate needs to be tailored accordingly using bespoke dissolution modulating additives. These modulators of Mg dissolution can be introduced into various protection schemas as part of an active protective coating or used as a component of the service environment in the case of Mg-air batteries. Consequently, benign degradation modulating additives need to be identified for all of these applications. In addition to a multitude of experimental high-throughput techniques that can be used to identify such compounds for light metal materials on comparably small timescales,[18-21] recent advances in computer technology facilitate the coupling of experimental discovering methods with computational techniques[22-23] to further accelerate the discovery process of novel compounds with useful properties. Furthermore, they greatly contribute to a comprehensive understanding of the underlying mechanisms.[24-26] There are two major strategies that can be adopted to identify compounds with suitable degradation modulating properties using computational techniques. The first is a data-driven machine learning (ML) approach[22,27-30] that is based on quantitative structure-activity relationships to predict the experimental performance of untested compounds. It could be demonstrated that this strategy exhibits great potential concerning the discovery and screening of large amounts of different molecules as the reported predictions are quite accurate. A prerequisite for a robust preselection of compounds with potentially useful properties based on this approach is the existence of sufficient training data as well as identification of sound molecular descriptors to train the underlying in silico models. Concomitantly, data-driven models cannot predict the performance of molecules exhibiting features outside of their domain (e.g., containing functional groups or substitution patterns that are not existing in the training set) reliably. A complementary second strategy for cases where promising compounds are already known either from a preceding in silico screening approach or based on their already demonstrated suitability for a specific application is to select one of these dissolution modulators as parent system. The properties of the selected molecule are subsequently tuned based on atomistic simulations (e.g., density functional theory calculations)[31-32] to tailor its effect on the dissolution of the material to a specific application, whereas this approach facilitates investigation of molecular features that are unknown to the previously mentioned ML models. It was shown that iron (Fe) plays a crucial role in the corrosion process of commercially pure (CPMg) and high-purity Mg (HPMg).[33-35] Hence, tuning the electronic properties of a given modulator by introducing electron donating (EDG) and electron withdrawing (EWG) functional moieties should impact its affinity to metal ions like Mg(II) and Fe(II)/(III) as well. Consequently, this approach facilitates a tailored degradation rate of the investigated materials. Here bipyridine was chosen as parent system, as its interaction with metal ions is well investigated[36-40] and it can be substituted with a large variety of functional groups following a comparably simple synthesis.[41]

Submitted for publication: May 27, 2020. Revised and accepted: July 27, 2020. Preprint available online: July 27, 2020, https://doi.org/10.5006/3597.
‡ Corresponding author. E-mail: christian.feiler@hzg.de.
* Magnesium Innovation Centre - MagIC, Institute of Materials Research, Helmholtz-Zentrum Geesthacht, Geesthacht, Germany 21502.
** Institute for Materials Science, Faculty of Engineering, Kiel University, Kiel, Germany 24143.

ISSN 0010-9312 (print), 1938-159X (online)

Table 1. *The Elemental Composition of High-Purity (HPMg51) and Commercially Pure Mg (CPMg342) Materials Used in This Study*[A]

Material	Element Content (wt%)										
	Fe	Cu	Ni	Al	Mn	Ce	Zn	Si	Ca	Zr	Mg
HPMg51	0.0051	<0.0001	<0.0002	0.0050	0.0008	<0.0004	0.0004	0.0053	<0.0001	0.0023	bal.
CPMg342	0.0342	0.0004	<0.0002	0.0040	0.0024	0.0007	0.0005	0.0007	<0.0001	<0.0005	bal.

[A] The number indicates the contained iron impurities in ppm. Balance is abbreviated as bal.

EXPERIMENTAL PROCEDURES

In vacuo density functional theory (DFT) calculations were performed using the TPSSh functional in combination with a def2SVP basis set using the quantum chemical software package Turbomole 7.2†.[42] After the geometry optimizations converged for an energy convergence criterion of 10^{-6}, frequency calculations were performed to ensure that minimum energy structures of the investigated systems were obtained. The basis set size was subsequently increased to def2TZVP and def2QZVP to prove that the comparably small double zeta basis is already sufficient to obtain accurate geometries while saving a substantial amount of computational costs (for details see the Supplemental Material). Continuous hydrogen evolution tests were performed to evaluate the degradation rate of magnesium in presence of various dissolution modulators. Analogous to previous studies, eudiometers (Art. Nr. 2591-10-500 from Neubert-Glas, Germany) were used for these investigations.[17,43] Water displaced by evolved hydrogen was automatically weighed (SKX† series from OHAUS coupled with USB data logger OHAUS 30268984†) and the data recorded for further processing using an in-house Python† script.[43] A flask below the eudiometer was filled with 500 mg of magnesium chips and 250 mL of electrolyte (0.5 wt% NaCl) without (reference) and with addition of a dissolution modulator. The reference value was determined from the normalized volume of hydrogen evolved after 20 h of immersion ($V_{Reference}$). This testing time is sufficient as the hydrogen evolution rate is in a steady state after ~10 h.[17,43] Subsequently, the chips were exposed to an electrolyte solution containing 0.01 M of dissolution modulator for 20 h, with the initial pH being adjusted by NaOH/HCl to 6.8±0.5 ($V_{Additive}$). The impact of the investigated modulator on the corrosion of magnesium is described by the inhibition efficiency (IE), which is determined according to the following equation:

$$IE[\%] = ((V_{Reference} - V_{Additive})/V_{Reference}) \times 10 \quad (1)$$

The elemental compositions of the two grades of pure magnesium that were used in this work are shown in Table 1. The values were determined by optical discharge emission spectroscopy (SPECTROLAB† with Spark Analyser Vision† software, Germany). The mean surface area of the used specimen was determined as 47.7±5.0 cm^2/g for the CPMg and as 111.7 ±10.7 cm^2/g for the HPMg material.

RESULTS AND DISCUSSION

It is well known that the performance of a corrosion modulator may be dependent on its concentration. Hence, concentration dependent measurements were performed for the inhibition efficiencies of the parent system 2,2′-bipyridine (bipy) for the two investigated materials (see Table 2). It is apparent that the dissolution modulator concentration does not significantly influence the measured inhibition efficiencies of bipy within a range of 10 mM to 40 mM. Hence, all subsequent experiments were performed at a concentration of 10 mM.

Table 2. *Impact of Used Inhibitor Concentration on the Inhibition Efficiencies for Two Pure Mg Materials*[A]

Bipy (mM)	Material			
	HPMg51		CPMg342	
	H_2 (mL)	IE %	H_2 (mL)	IE %
Ref.	18.0	0	382.0	0
50	precipitates		precipitates	
40	12.9±1.1	28±6	220.6±15.0	42±4
25	13.1±0.8	27±4	281.8±13.3	26±3
10	13.0±2.0	28±11	266.9±2.9	30±1

[A] Each value is the mean of three replicates. A reference value (Ref.) for the amount of evolved hydrogen in absence of a dissolution modulator is provided.

Complexes of bipyridine-type ligands with metal ions are based on the interaction between the lone pair of the nitrogen with a metal ion. Substitution of the parent system with EWGs and EDGs influences the electron density of the bipy's on the nitrogen atoms. Concomitantly, this approach facilitates tailoring the strength of the formed coordinative bond between nitrogen atom and metal ion for a specific target requirement.[32,44]

The four 2,2′-bipyridine derivatives that exhibit a symmetric substitution pattern are depicted in Figure 1. However, the 6,6′-derivative **1** will not form complexes with a metal due to strong intermolecular repulsion (light blue arcs) between neighboring ligands upon formation of the 3:1 complex (Figure 1, right). The 5,5′ derivatives of 2,2′-bipyridine (**2**) were also not considered here as substitution in meta position does not have a significant effect on the electron density of the nitrogen atoms. For the same reason, the electronic effect on 3,3′-substituted 2,2′ bipyridines (**4**) is not pronounced. Furthermore, introduction of functional groups at this position will lead to distinct intramolecular interaction (orange arcs) with the functional group on the neighboring pyridine ring. The forced geometry of compound **4** further weakens its capability to form complexes. Contrary to this, the 4,4′-substituted derivative **3** will not impair complexation of metal ions. Additionally, the introduction of EWGs and EDGs in para position of the pyridine ring exhibits a pronounced effect on the nitrogen atom in the pyridine ring. Hence, 4,4′-substituted 2,2′-bipyridines **3** (see Figure 1) as leitmotif were selected for the study. Subsequently, five

† Trade name.

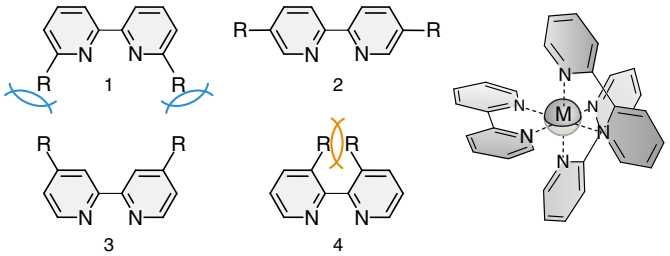

FIGURE 1. *The four symmetric substitution patterns of 2,2′-bipyridine. Intermolecular interactions caused by formation of the 3:1 complex with a metal ion (right) are depicted as light blue arcs. Intramolecular interactions are represented as orange arcs.*

derivatives of the parent system **3** (R = H) were selected and the charge ($\delta_{Py\text{-}N}$) of the nitrogen atom was determined based on quantum chemical calculations and a subsequent natural bond orbital (NBO) analysis at the TPPSh/def2SVP level of DFT. Introduction of a methyl group does not have a distinct effect. Substitution with electron donating methoxy (OCH_3-bipy) or dimethylamino ($N(CH_3)_2$-bipy) moieties leads to a significant increase in partial negative charge, whereas introduction of electron withdrawing carboxylic acid (COOH-bipy) or methyl carboxylate ($COOCH_3$-bipy) groups causes a considerably less negative partial charge on the nitrogen atom in the pyridine ring (see Figure 2). It is noteworthy that the computed $\delta_{Py\text{-}N}$ values correlate quite well ($R^2 = 0.94$) with the Hammett parameters (σ_{para}) that were determined for the investigated functional groups.[45]

Subsequently the octahedral complexes that are formed by three bipyridine ligands with the metal ions of interest (Mg(II) and Fe(II)) were modeled. These two metal ions were chosen for the computational study as increased complexation of Mg ions will naturally result in higher degradation rates of the material if a soluble complex is formed, whereas weaker affinities to Mg should lead to less corrosion acceleration. Furthermore, the interaction of the dissolution modulator with iron ions is expected to play a crucial role in the degradation process of HPMg and CPMg as re-plating of the noble impurity will cause further acceleration of the corrosion rate.[17,33-35,46] Consequently, it is important to consider the corresponding complexes that are formed with bipy-type ligands. Here only Mg(II) and Fe(II) complexes are investigated as complex formation of bipy and Fe(II) will prevent further oxidation to Fe(III) as the corresponding complex ($[Fe(III)\text{-}(bipy)_3]^{3+}$) is unstable.[47] All complexes of the six potential candidates with Mg(II) and Fe(II) have been geometry optimized at the TPSSh/def2SVP level of DFT. However, the description of the electronic structure of iron complexes is highly challenging and often inconsistent as different levels of theory and experimental techniques will identify various electronic ground states for the same compound.[48-51] The situation is even more complicated as iron complexes may adopt three different spin states (low spin, intermediate spin, high spin), whereas each respective ground state may consist of mixed electronic configurations resulting in highly controversial discussions over the last decades.[52-53] According to the geometry optimizations on the TPSSh/def2SVP level of DFT all complexes of the investigated bipy parent system and its derivatives with Fe(II) are most stable in the low spin state. This is in good agreement with other works on $[Fe(II)\text{-}(bipy)_3]^{2+}$, as the three bipyridine ligands induce a strong ligand field. Consequently, the diamagnetic low spin state is energetically more favorable for the homoleptic complex[36-38] and the spin crossover to the high spin state cannot be induced thermally under ambient conditions.[54] Fortunately, it has been demonstrated that DFT methods can describe the geometry of such transition metal complexes quite well, although the obtained energies may not be accurate.[32,55-56] Consequently, it is assumed that the distance between metal center and coordinating nitrogen of the investigated bipyridines is indicative of the degree of interaction between ligands and the

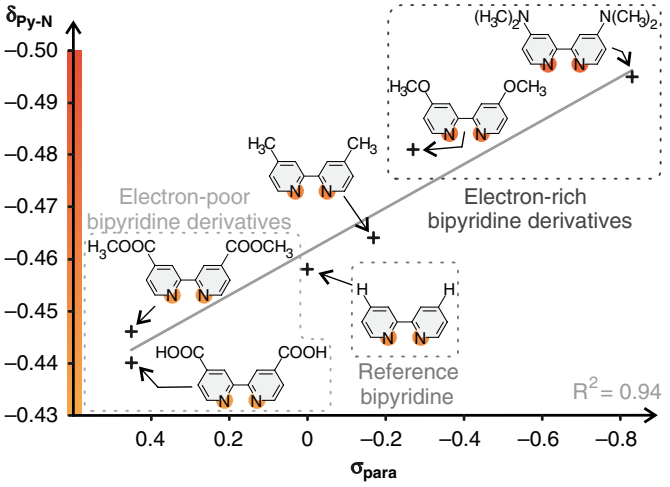

FIGURE 2. *Color-coded representation of the mean of the partial negative charge ($\delta_{Py\text{-}N}$) located on the nitrogen atoms of bipyridine (bipy) and five derivatives against their corresponding Hammett parameters (σ_{para}). Introduction of electron withdrawing groups (COOH, $COOCH_3$) in para position decreases the negative partial charge, while substitution with electron donating groups (OCH_3, $N(CH_3)_2$) increases the negative partial negative charge on the nitrogen atom in comparison to the parent system. A linear least square fit (gray) is included as guide for the eye.*

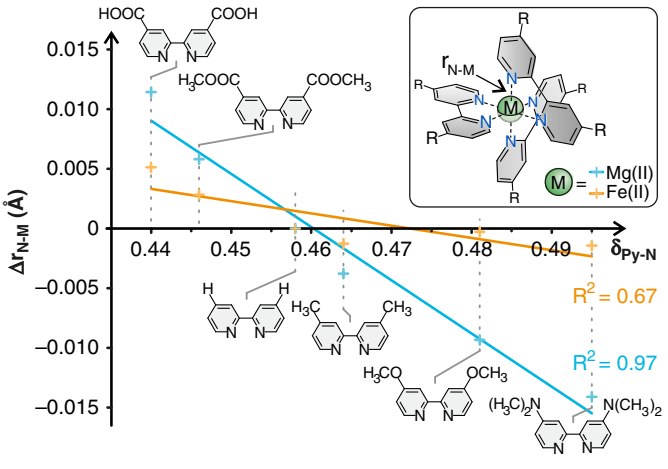

FIGURE 3. *Mean distance between the six nitrogen atoms and the central metal atom in the calculated 3:1 complexes with Mg(II) (light blue) and Fe(II) (orange) ions relative to the parent system. Linear least square fits in corresponding colors are shown as guide for the eye. Shorter distances indicate stronger interaction with the investigated metal ions relative to the parent system. The inlay (top right) shows a general representation of the homoleptic 3:1 complex that was used as basis to determine the distance ($r_{N\text{-}M}$) between the central metal ion and the coordinating nitrogen atom. The substitute symbol R depicts the functionalization in para position of the pyridine ring.*

complexed metal cation (see Figure 3). A stronger interaction between dissolution modulator and metal ion will result in a shorter N-M distance and vice versa. Note that the low spin structures of the respective complexes were used to quantify the interaction of bipy and its derivatives with Fe(II).

The theoretical investigation indicates that introduction of EWGs and EDGs in 4,4′ position of bipy should have an insignificant influence on the interaction strength with Fe(II) ions. The determined distances show a modest correlation (R^2 = 0.67) with the partial negative charges on the nitrogen atoms. However, the N-M distances obtained from the quantum chemical calculations express a slight trend toward a stronger interaction of the electron-rich bipy derivatives with iron. According to the calculations, the complexation strength should decrease in the order R = $N(CH_3)_2$ ≈ CH_3 > OCH_3 > H > $COOCH_3$ > COOH. Contrary to the minor effect on the complexation strength of Fe(II), the structures of the corresponding complexes with Mg(II) exhibit significant differences regarding the distance between nitrogen atom of bipy and Mg(II). The length of the coordinative bond decreases in the order R = $N(CH_3)_2$ > OCH_3 > CH_3 > H > $COOCH_3$ > COOH and the calculated distances show a distinct correlation with an R^2 of 0.97. This indicates that electron-rich bipy derivatives accelerate the degradation of Mg-based materials, while their electron-poor counterparts have a corrosion-inhibiting effect with respect to the parent system. This trend is further corroborated by the complex formation energies (ΔE_f) calculated using the TPSSh functional in combination with all three investigated basis sets as ΔE_f decreases in the order R = $N(CH_3)_2$ > OCH_3 > CH_3 > H > $COOCH_3$ > COOH for the investigated complexes with Mg(II). Concomitantly, Δr_{N-M} correlates quite well with the calculated ΔE_f, whereas the respective linear least square fits exhibit R^2 values of 0.96 (TPSSh/def2SVP), 0.98 (TPSSh/def2TZVP), and 0.97 (TPSSh/def2QZVP). This finding complements the claims that r_{N-M} is indicative of the interaction strength of bipy-type dissolution modulators with Mg and that the comparably small def2SVP basis set already yields sufficiently accurate results while imposing substantially lower computational costs (for details see the Supplemental Material). To validate the prediction of the theoretical investigation, hydrogen evolution experiments were performed under the same conditions that were used for the reference system based on two different grades of pure magnesium (HPMg51 and CPMg342). Note that the dimethylamino-derivative ($N(CH_3)_2$-bipy) as well as the methyl acetate-functionalized bipyridine (COOCH3-bipy) were excluded from the experimental investigation as these compounds are highly expensive (100 mg cost more than 400 €) and hence, not likely to be incorporated in practical applications. Furthermore, the experimental investigation of the methyl-functionalized bipyridine was unsuccessful as this ligand is insoluble at the used concentration. The experimental results of the parent system as well as its two remaining derivatives (OCH_3-bipy and COOH-bipy) are shown in Table 3.

COOH-bipy performs equally well for both materials and acts as inhibiting agent in comparison to the parent system, whereas dissolution of both materials is accelerated in presence of OCH_3-bipy in comparison to the other two compounds. The acceleration effect is more pronounced for the HPMg51 substrate than for CPMg342 as the latter is highly sensitive to Fe-complexing ligands due to the high level of Fe impurities. As previously mentioned, OCH_3-bipy should also form slightly stronger complexes with Fe(II), which is a positive factor concerning the corrosion inhibition of Mg.[17,34,46] The minor effect on the complexation of iron seems to be the reason for the weak inhibiting effect of OCH_3-bipy on the dissolution of CPMg342 in comparison to its effect on the high-purity material. However, the distinctly stronger interaction with Mg(II) ions still shifts the equilibrium toward the dissolution of CPMg342 in comparison to the parent system. On the contrary, the level of Fe impurities is very low in HPMg51, thus the partial corrosion-inhibiting effect of OCH_3-bipy that is caused by the slightly elevated interaction strength with Fe is not countering its dissolution accelerating effect caused by stronger binding of Mg(II). Taking the minor effect on the complexation of iron into account provides a sound argument for the more negative values of IE for HPMg51 as well as the slightly positive values of IE for CPMg342 in presence of OCH_3-bipy. Nevertheless, the inhibition efficiency decreases for both materials in the order COOH-bipy > bipy > OCH_3-bipy, which is in good agreement with the trend predicted based on the length of the coordinative bonds to Mg (see Figure 3).

Table 3. *Inhibiting Efficiencies of Bipyridine as well as Two Derivatives*[(A)]

		Material			
		HPMg51		CPMg342	
Additive	(mM)	H_2 (mL)	IE %	H_2 (mL)	IE %
Ref.	0	18.0	0	382.0	0
OCH_3-bipy	10	22.7±4.4	-26±24	318.3±10.6	17±3
bipy	10	13.0±2.0	28±11	266.9±2.9	30±1
COOH-bipy	10	3.6±0.4	80±2	68.6±1.8	82±1

[(A)] The amount of evolved hydrogen in absence of a dissolution modulating agent is provided as reference (Ref.). Each of the provided values is the mean of three replicates. The third derivative (CH_3-bipy) that was investigated experimentally precipitated at the used concentration and is therefore not listed in the table.

CONCLUSIONS

➢ In the scope of the presented work a correlation between the coordinative bond length of the investigated bipyridine derivatives to magnesium ions and the corrosion behavior of two grades of pure magnesium was identified. A computational study on the complexes formed by 2,2′-bipyridine and five of its derivatives with magnesium and iron was conducted to elucidate the effect of electron withdrawing and electron donating functional groups on the complex formation with the two metal ions.

➢ The theoretical prediction was subsequently validated by hydrogen evolution experiments using dissolution modulator concentrations of 10 mM, as it could be demonstrated that the corrosion inhibition efficiencies of the parent system bipyridine are concentration independent between 10 mM and 40 mM.

➢ The presented approach is highly promising strategy to tailor the performance of other potential dissolution modulators to the requirements of target applications ranging from engineering applications (corrosion inhibition) over biomedical applications (slow degradation) to battery applications that require constant dissolution of Mg-based anode material. However, a prerequisite to follow this approach for other compounds of interest is that they can be synthetically modified with functional moieties that influence the interaction with metal ions of interest.

➢ The findings presented in this work indicate that this strategy is a promising complementary approach to the data-driven performance prediction of potential dissolution modulating agents using machine learning techniques,[22,28-30] as it is computationally inexpensive, robust, and requires significantly less data. Concomitantly, the investigated bond length depicts a promising molecular descriptor for the training of predictive quantitative structure-activity/property relationship (QSAR/QSPR) models concerning the anticorrosive effect of small organic molecule additives provided that all compounds in the used dataset are sensitive to this parameter. Furthermore, the presented approach facilitates a post processing step of potential candidates that were preselected by machine learning methods.

ACKNOWLEDGMENTS

Funding by HZG MMDi IDEA project is gratefully acknowledged. DM thanks China Scholarship Council for the award of fellowship and funding (No. 201607040051). The authors declare no competing financial interest.

References

1. W.J. Joost, P.E. Krajewski, *Scr. Mater.* 128 (2017): p. 107-112.
2. C. Blawert, N. Hort, K.U. Kainer, *Trans. Indian Inst. Met.* 57 (2004): p. 397-408.
3. H. Friedrich, S. Schumann, *J. Mater. Process. Technol.* 117 (2001): p. 276-281.
4. J. Hirsch, T. Al-Samman, *Acta Mater.* 61 (2013): p. 818-843.
5. A.A. Luo, *J. Magnesium Alloys* 1 (2013): p. 2-22.
6. A. Dziubińska, A. Gontarz, M. Dziubiński, M. Barszcz, *Adv. Sci. Technol. Res. J.* 10 (2016): p. 158-168.
7. M. Gupta, N. Gupta, *Aeron. Aero. Open Access J.* 1 (2017): p. 41-46.
8. B.J.C. Luthringer, F. Feyerabend, R. Willumeit-Römer, *Magnes. Res.* 27 (2014): p. 142-154.
9. A. Santos-Coquillat, M. Esteban-Lucia, E. Martinez-Campos, M. Mohedano, R. Arrabal, C. Blawert, M.L. Zheludkevich, E. Matykina, *Mater. Sci. Eng. C* 105 (2019): p. 110026.
10. C. Shuai, S. Li, S. Peng, P. Feng, Y. Laid, C. Gao, *Mater. Chem. Front.* 3 (2019): p. 544-562.
11. C. Rapetto, M. Leoncini, *J. Thorac. Dis.* (2017): p. S903-S913.
12. D. Höche, S.V. Lamaka, B. Vaghefinazari, T. Braun, R. Petrauskas, M. Fichtner, M.L. Zheludkevich, *Sci. Rep.* 8 (2018): p. 7578.
13. H.D. Yoo, J.R. Jokisaari, Y.-S. Yu, B.J. Kwon, L. Hu, S. Kim, S.-D. Han, M. Lopez, S.H. Lapidus, G.M. Nolis, B.J. Ingram, I. Bolotin, S. Ahmed, R.F. Klie, J.T. Vaughey, T.T. Fister, J. Cabana, *ACS Energy Lett.* 4 (2019): p. 1528-1534.
14. Y. Zhang, M. Konya, A. Kutsuma, S. Lim, T. Mandai, H. Munakata, K. Kanamura, *Small* 15 (2019): p. 1902236.
15. M. Esmaily, J.E. Svensson, S. Fajardo, N. Birbilis, G.S. Frankel, S. Virtanen, R. Arrabal, S. Thomas, L.G. Johansson, *Prog. Mater. Sci.* 89 (2017): p. 92-193.
16. H. Liu, F. Cao, G.-L. Song, D. Zheng, Z. Shi, M.S. Dargusch, A. Atrens, *J. Mater. Sci. Technol.* 35 (2019): p. 2003-2016.
17. S.V. Lamaka, B. Vaghefinazari, D. Mei, R.P. Petrauskas, D. Höche, M.L. Zheludkevich, *Corros. Sci.* 128 (2017): p. 224-240.
18. S.J. García, T.H. Muster, Ö. Özkanat, N. Sherman, A.E. Hughes, H. Terryn, J.H.W. de Wit, J.M.C. Mol, *Electrochim. Acta* 55 (2010): p. 2457-2465.
19. P.A. White, G.B. Smith, T.G. Harvey, P.A. Corrigan, M.A. Glenn, D. Lau, S.G. Hardin, J. Mardel, T.A. Markley, T.H. Muster, N. Sherman, S.J. Garcia, J.M.C. Mol, A.E. Hughes, *Corros. Sci.* 58 (2012): p. 327-331.
20. T.H. Muster, A.E. Hughes, S.A. Furman, T. Harvey, N. Sherman, S. Hardin, P. Corrigan, D. Lau, F.H. Scholes, P.A. White, M. Glenn, J. Mardel, S.J. Garcia, J.M.C. Mol, *Electrochim. Acta* 54 (2009): p. 3402-3411.
21. M. Meeusen, L. Zardet, A.M. Homborg, M. Lekka, F. Andreatta, L. Fedrizzi, B. Boelen, H. Terryn, J.M.C. Mol, *J. Electrochem. Soc.* 166 (2019): p. C3220-C3232.
22. D.A. Winkler, M. Breedon, P. White, A.E. Hughes, E.D. Sapper, I. Cole, *Corros. Sci.* 106 (2016): p. 229-235.
23. P.A. White, G.E. Collis, M. Skidmore, M. Breedon, W.D. Ganther, K. Venkatesan, *New. J. Chem.* 44 (2020): p. 7647-7658.
24. J.A. Yuwono, C.D. Taylor, G.S. Frankel, N. Birbilis, S. Fajardo, *Electrochem. Commun.* 104 (2019): p. 106482.
25. I. Milošev, D. Zimerl, C. Carriére, S. Zanna, A. Seyeux, J. Iskra, S. Stavber, F. Chiter, M. Poberžnik, D. Costa, A. Kokalj, P. Marcus, *J. Electrochem. Soc.* 167 (2020): p. 061509.
26. M. Poberžnik, F. Chiter, I. Milošev, P. Marcus, D. Costa, A. Kokalj, *Appl. Surf. Sci.* 525 (2020): p. 146156.
27. D.A. Winkler, *Metals* 7 (2017): p. 553-561.
28. T. Würger, C. Feiler, F. Musil, G.B.V. Feldbauer, D. Höche, S.V. Lamaka, M.L. Zheludkevich, R.H. Meißner, *Front. Mater.* 6 (2019): p. 53.
29. C. Feiler, D. Mei, B. Vaghefinazari, T. Würger, R. Meißner, B. Luthringer-Feyerabend, D.A. Winkler, M.L. Zheludkevich, S.V. Lamaka, *Corros. Sci.* 163 (2020): p. 108245.
30. T.L.P. Galvão, G. Novell-Leruth, A. Kuznetsova, J. Tedim, J.R.B. Gomes, *J. Phys. Chem. C* 124 (2020): p. 5624-5635.
31. M. Dommaschk, C. Schütt, S. Venkataramani, U. Jana, C. Näther, F.D. Sönnichsen, R. Herges, *Dalton Trans.* 43 (2014): p. 17395-17405.
32. C. Schütt, G. Heitmann, T. Wendler, B. Krahwinkel, R. Herges, *J. Org. Chem.* 81 (2016): p. 1206-1215.
33. D. Höche, C. Blawert, S.V. Lamaka, N. Scharnagl, C. Mendis, M.L. Zheludkevich, *Phys. Chem. Chem. Phys.* 18 (2016): p. 1279-1291.
34. S.V. Lamaka, D. Höche, R.P. Petrauskas, C. Blawert, M.L. Zheludkevich, *Electrochem. Commun.* 62 (2016): p. 5-8.
35. D. Mercier, J. Światowska, S. Zanna, A. Seyeux, P. Marcus, *J. Electrochem. Soc.* 165 (2018): p. C42-C49.
36. Y. Saito, J. Takemoto, B. Hutchins, K. Nakamoto, *Inorg. Chem.* 11 (1972): p. 2003.
37. P. Gütlich, Y. Garcia, H.A. Goodwin, *Chem. Soc. Rev.* 29 (2000): p. 419-427.
38. D.N. Bowman, E. Jakubikova, *Inorg. Chem.* 51 (2012): p. 6011-6019.
39. A.K. Das, R.V. Solomon, F. Hofmann, M. Meuwly, *J. Phys. Chem. B* 120 (2016): p. 206-216.
40. J. Karges, G. Gasser, *Synthesis Inorg. Chim. Acta* 499 (2020): p. 119196.
41. M. Heller, U.S. Schubert, *J. Org. Chem.* 67 (2002): p. 8269-8272.
42. TURBOMOLE V7.2 (2018), a development of University of Karlsruhe and Forschungszentrum Karlsruhe GmbH, 1989-2019, TURBOMOLE GmbH, since 2007; available from http://www.turbomole.com.
43. D. Mei, S.V. Lamaka, C. Feiler, M.L. Zheludkevich, *Corros. Sci.* 153 (2019): p. 258-271.
44. M. Dommaschk, M. Peters, F. Gutzeit, C. Schütt, C. Näther, F.D. Sönnichsen, S. Tiwari, C. Riedel, S. Boretius, R. Herges, *J. Am. Chem. Soc.* 137 (2015): p. 7552-7555.
45. C. Hansch, A. Leo, R.W. Taft, *Chem. Rev.* 91 (1991): p. 165-195.
46. A. Maltseva, S.V. Lamaka, K.A. Yasakau, D. Mei, D. Kurchavov, M.L. Zheludkevich, G. Lefèvre, P. Volovitch, *Corros. Sci.* (2020): p. 108484.
47. A.M. Josceanu, P. Moore, *J. Chem. Soc. Dalton Trans.* (1998): p. 369-374.
48. M. Gruyters, T. Pingel, T.G. Gopakumar, N. Néel, C. Schütt, F. Köhler, R. Herges, R. Berndt, *J. Phys. Chem. C* 116 (2012): p. 20882-20886.
49. M. Swart, M. Gruden, *Acc. Chem. Res.* 49 (2016): p. 2690-2697.
50. K.P. Keep, *Commun. Chem.* 61 (2018): p. 1.
51. B. Pinter, A. Chankisjijev, P. Geerlings, J.N. Harvey, F. De Proft, *Chem. Eur. J.* 24 (2018): p. 5281-5292.
52. J. Fernández-Rodríguez, B. Toby, M. van Veenendaal, *Phys. Rev. B* 91 (2015): p. 214427.
53. S. Stepanow, P.S. Miedema, A. Mugarza, G. Ceballos, P. Moras, J.C. Cezar, C. Carbone, F.M.F. de Groot, P. Gambardella, *Phys. Rev. B* 83 (2011): p. 220401.
54. L. Daku, A. Hauser, *J. Phys. Chem. Lett.* 1 (2010): p. 1830-1835.
55. M. Dommaschk, V. Thoms, C. Schütt, C. Näther, R. Puttreddy, K. Rissanen, R. Herges, *Inorg. Chem.* 54 (2015): p. 9390-9392.
56. M. Klaß, J. Krahmer, C. Näther, F. Tuczek, *Dalton Trans.* 47 (2018): p. 1261-1275.